ISSN 1995-4239, Numerical Analysis and Applications, 2017, Vol. 10, No. 1, pp. 28–36. © Pleiades Publishing, Ltd., 2017.
Original Russian Text © H.Sh. Mahato, 2017, published in Sibirskii Zhurnal Vychislitel'noi Matematiki, 2017, Vol. 20, No. 1, pp. 37–46.

Numerical Simulations for a Two-Scale Model in a Porous Medium

H. Sh. Mahato*

College of Engineering, University of Georgia, 30602 Athens, USA

Received November 24, 2015; in final form, July 5, 2016

Abstract—This paper deals with the numerical simulations of a system of diffusion-reaction equations in the context of a porous medium. We start by giving a microscopic model and then the upscaled version (i.e., homogenized or continuum model) of it from the previous works of the author. Since with the help of homogenization we obtain the macroscopic description of a model that is microscopically heterogeneous, via these numerical simulations, we show that this macroscopic description approximates the microscopic model, which contains the heterogeneities and oscillating terms at the pore scale such as diffusion coefficients.

DOI: 10.1134/S1995423917010049

Keywords: *periodic medium, two-scale model, averaging, numerical simulations*.

1. INTRODUCTION

In this chapter, a mathematical model is investigated numerically. For the sake of illustration, we restrict ourselves to 2-dimensional situations. All the figures in this paper are generated by the author by conducting numerical simulations in COMSOL Multiphysics 4.3a. (see [1]). To illustrate the problem, let us start by the modeling first. As we know that many problems in the fields of physics, chemistry, biology and engineering sciences are governed by *diffusion-reaction equations*. One of the most vital phenomena that can be explained with the help of these equations is the chemical transport in porous media (e.g., in soil, concrete, reservoir, rock, etc.), cf. [3, 9]. Let $\Omega \subset \mathbb{R}^n$, where $n = 2$, be a perforated porous medium under consideration and $Y := (0,1)^n \subset \mathbb{R}^n$ be a unit representative cell. Further assume that

- $Y = Y_s \cup Y_p$, where the solid part Y_s with boundary Γ and the pore part Y_p in Y are such that $\bar{Y_s} \subset Y$ and $\bar{Y_s} \cap Y_p = \phi$;
- Ω is composed of a pore space Ω_p and the union of disconnected solid parts Ω_s such that $\Omega := \Omega_p \cup \Omega_s$ and $\Omega_p \cap \bar{\Omega}_s = \phi$. Γ^* and $\partial\Omega$ are the union of boundaries of solid parts and the outer boundary of Ω. Ω is periodic (i.e., the solid parts in Ω are periodically distributed) and is covered by a finite union of the cells $Y_k := Y + k,\ k \in \mathbb{Z}^n$. $Y_{p_k} := Y_p + k$, $Y_{s_k} := Y_s + k$ and $\Gamma_k := \Gamma + k$, $k \in \mathbb{Z}^n$;
- for a scale parameter $\varepsilon > 0$, we denote the pore space, solid parts and the union of the boundaries of solid matrices in Ω by Ω_p^ε, Ω_s^ε and Γ^ε and they are defined as: $\Omega_p^\varepsilon := \bigcup_{k\in\mathbb{Z}^n} \{\varepsilon Y_{p_k} : \varepsilon Y_{p_k} \subset \Omega\}$, $\Omega_s^\varepsilon := \bigcup_{k\in\mathbb{Z}^n} \{\varepsilon Y_{s_k} : \varepsilon Y_{s_k} \subset \Omega\}$, and $\Gamma^\varepsilon := \bigcup_{k\in\mathbb{Z}^n} \{\varepsilon \Gamma_k : \varepsilon \Gamma_k \subset \Omega\}$;
- the boundaries $\Gamma, \Gamma^*, \Gamma^\varepsilon, \partial\Omega \in C^2$. We denote by dx and dy the volume elements in Ω and Y, and by $d\sigma_y$ and $d\sigma_x$ the surface elements on Γ and Γ^ε, respectively;

*E-mail: hsmahato@uga.edu

- for a $T > 0$, $S := [0, T)$ be the time interval. We denote $\mathbb{R}^+ := \{x \in \mathbb{R} : x > 0\}$, $\mathbb{R}_0^+ := \mathbb{R}^+ \cup \{0\}$, $\mathbb{N} = \{1, 2, 3, \ldots\}$, and $\mathbb{N}_0 := \mathbb{N} \cup \{0\}$.

The required model under investigation at the micro scale is given by

$$\frac{\partial u_\varepsilon}{\partial t} - \nabla \cdot D\nabla u_\varepsilon = \mathcal{M}R(u_\varepsilon) \quad \text{in} \quad (0,T) \times \Omega_p^\varepsilon, \tag{1.1}$$

$$u_\varepsilon(0,x) = u_0(x) \quad \text{in} \quad \Omega_p^\varepsilon, \tag{1.2}$$

$$-D\nabla u_\varepsilon \cdot \vec{n} = 0 \quad \text{on} \quad (0,T) \times \partial\Omega, \tag{1.3}$$

$$-D\nabla u_\varepsilon \cdot \vec{n} = 0 \quad \text{on} \quad (0,T) \times \Gamma^\varepsilon. \tag{1.4}$$

We denote this problem by (P_ε). Here $D = \text{diag}(d_1, d_2, \ldots, d_I)$ is a diagonal matrix of diffusion coefficients and $u_\varepsilon := (u_{\varepsilon_1}, u_{\varepsilon_2}, \ldots, u_{\varepsilon_I})$ is the vector of molar concentrations of $I\,(\in \mathbb{N})$ chemical species involved in $J(\in \mathbb{N})$ reactions given by

$$\tau_{1j}X_1 + \tau_{2j}X_2 + \ldots + \tau_{Ij}X_I \rightleftharpoons \nu_{1j}X_1 + \nu_{2j}X_2 + \ldots + \nu_{Ij}X_I, \quad 1 \le j \le J, \tag{1.5}$$

where X_i, $1 \le i \le I$, denotes the chemical species and the stoichiometric coefficients $\tau_{ij}, \nu_{ij} \in \mathbb{N}_0$. Set the stoichiometric matrix $\mathcal{M} := (s_{ij})_{\substack{1 \le i \le I \\ 1 \le j \le J}}$, where $s_{ij} = \nu_{ij} - \tau_{ij}\, \forall i, j$. The reaction rate for the ith species, via mass-action kinetics, is given by

$$(\mathcal{M}R(u_\varepsilon))_i = \sum_{j=1}^{J} s_{ij} \left(k_j^f \prod_{\substack{m=1 \\ s_{mj}<0}}^{I} (u_{\varepsilon_m})^{-s_{mj}} - k_j^b \prod_{\substack{m=1 \\ s_{mj}>0}}^{I} (u_{\varepsilon_m})^{s_{mj}} \right) \ \forall i = 1, 2, \ldots, I, \tag{1.6}$$

where k_j^f and k_j^b are forward and backward reaction rate factors. For this model, we solve the micro problem, the cell-problems, and the macro problem, respectively. Obviously, the problem at micro scale describes the heterogeneities present in the medium but it fails to give global behavior of the model and numerical simulation will lead to a cumbersome analysis as to catch these micro heterogeneities the size of the step-length involved in numerical simulation should be chosen so small such that it can catch those micro heterogeneities. This will lead to a huge time consumption by the computer. In case of the real world problems where lot of parameters are involved, the numerical simulations does not seem to fit well and therefore we would require the macroscopic description of the model, which provides the global behavior of the medium, involves no heterogeneities from the micro scale and helps to do numerical simulations without consuming too much time. By homogenization (i.e., upscaling or averaging), we basically look for a function u such that $\lim_{\varepsilon \to 0} u_\varepsilon = u$, however, while upscaling a mathematical model from the micro scale to the macro scale following questions needs to be answered:

- does there at all exist a function u s.t. u_ε converges to u?
- if that is true, in which sense the "*limit*" is taken and which function space does u belong to?
- does u solve some limit boundary value problem?
- what can be said about the diffusion coefficients of the limit problem?
- is u_ε an approximation of u?
- finally, do the upscaled models better suited for numerical simulations?

To answer the first three questions, we refer to the previous two papers of the author, e.g., [3, 4], however, to address the last three questions we verify that by conducting some numerical simulation, which is the main essence of this manuscript. We first start with the previous results of the author from [3, 4], which lay down the groundwork for the numerics done in this work. Let $p > n+2$ be such that $\frac{1}{p}+\frac{1}{q}=1$ and $\theta \in [0,1]$. Assume that $\Xi \in \{\Omega, \Omega_p^\varepsilon\}$, then $L^p(\Xi)$, $H^{1,p}(\Xi)$, $C^\theta(\Xi)$, $(\cdot,\cdot)_{\theta,p}$, $[\cdot,\cdot]_\theta$ and $C^\gamma_{\rm per}(Y)$ are the Lebesgue, Sobolev, Hölder, real interpolation, complex interpolation and Y-periodic γ times ($\gamma \in \mathbb{N}$) continuously differentiable function spaces, respectively, endowed with their standard norms. In particular, $C_{\rm per}(Y)$ is the space of all Y-periodic continuous functions in y. The *Sobolev–Bochner spaces* are given by $\mathcal{F}_p(\Xi) := \left\{u \in L^p(S;H^{1,p}(\Xi)) : \frac{du}{dt} \in L^p(S;H^{1,q}(\Xi)^*)\right\} = H^{1,p}(S;H^{1,q}(\Xi)^*) \cap L^p(S;H^{1,p}(\Xi))$ and have the norm

$$||u||_{\mathcal{F}_p(\Xi)} := ||u||_{L^p(S;H^{1,p}(\Xi))} + ||u||_{L^p(S;H^{1,q}(\Xi)^*)} + \left|\left|\frac{du}{dt}\right|\right|_{L^p(S;H^{1,q}(\Xi)^*)}, \tag{1.7}$$

whereas the norm on the vector-valued function spaces are defined as $|||u|||_{[\mathcal{F}_p(\Xi)]^I} := [\sum_{i=1}^{I} ||u_i||^p_{\mathcal{F}_p(\Xi)}]^{\frac{1}{p}}$. In particular, $|||u|||_{L^\infty(\Xi)^I} = \max\limits_{1\le i\le I} ||u_i||_{L^\infty(\Xi)}$. For further definitions of function spaces, embedding theorems and appropriate function space setting for the problem (P_ε), please confer to the work in [3]. Taking the assumptions of Theorem 2.1 in [3] on account, we have following

Theorem 1.1 (Existence theorem). *There exists a unique positive global weak solution $u_\varepsilon \in \mathcal{F}_p^I(\Omega_p^\varepsilon) \cap L^\infty(S\times\Omega_p^\varepsilon)^I$ of the problem (P_ε) and it satisfies the following estimate*:

$$\sup_{\varepsilon>0}\left(|||u_\varepsilon|||_{L^r((0,T);L^r(\Omega_\varepsilon^p))^I} + |||u_\varepsilon|||_{L^\infty((0,T);L^\infty(\Omega_\varepsilon^p))^I} + |||\nabla u_\varepsilon|||_{L^2((0,T);L^2(\Omega_\varepsilon^p))^I}\right) \le C < \infty, \tag{1.8}$$

where r is any arbitrarily chosen large positive integer and the constant C is independent of ε, t, and u^ε.

Theorem 1.1 is proved in [3]. The ingredients for the proof are an entropy function, Schaefer's fixed point theorem and Theorem 2.5 from [8], which is based on the maximal regularity of differential operators. In the proof of Theorem 1.1, it is being assumed that the diffusion coefficients are positive constant in t and x, to be precise, $d_1 = d_2 = \ldots = d_I = d > 0$. Nevertheless, it is worth mentioning that it has been known for quite some time that for systems of type (1.1) with different diffusion coefficients, the results concerning the existence of global weak solution are still unknown. A nice survey of such results can be found in [7] and recently for some particular type of reaction rates significant work has been done in [2, 5].

Now by the extension Theorem 4.2.1 in [4], estimate (1.8) can be extended in to all of $S\times\Omega$, i.e.,

$$\sup_{\varepsilon>0}\left(|||u_\varepsilon|||_{L^r((0,T);L^r(\Omega))^I} + |||u_\varepsilon|||_{L^\infty((0,T);L^\infty(\Omega))^I} + |||\nabla u_\varepsilon|||_{L^2((0,T);L^2(\Omega))^I}\right) \le C < \infty, \tag{1.9}$$

where the constant C is independent of ε, t, and u_ε. Also by a straightforward calculation one can obtain $\left|\left|\left|\chi^\varepsilon \frac{\partial u_\varepsilon}{\partial t}\right|\right|\right|_{L^2((0,T);H^{1,2}(\Omega)^*)^I}$. Therefore, by Theorem 2.1 in [6], we obtain that u_ε, up to a subsequence, is strongly convergent to a limit $u \in L^2(S\times\Omega)^I$.

Under the similar assumptions as in [3], by the homogenization techniques it has been shown in [4, Section 4 (in part., Subsection 4.3) and Thm. 4.11] that:

Theorem 1.2 (Upscaled problem). *There exists a unique $u \in \mathcal{F}_p^I(\Omega) \cap L^\infty(S\times\Omega)^I$, which satisfies the homogenized problem of (P_ε) given by*

$$\frac{\partial u}{\partial t} - \nabla\cdot\Upsilon\,\nabla u = SR(u) \quad \text{in} \quad (0,T)\times\Omega, \tag{1.10}$$

$$-\Upsilon\ \nabla u \cdot \vec{n} = 0 \quad \text{on} \quad (0,T) \times \partial\Omega, \tag{1.11}$$

$$u(0,x) = u_0(x) \quad \text{in} \quad \Omega. \tag{1.12}$$

Here $\Upsilon = (\beta_{jk})_{1\le j,k\le 2}$ *is a second-order tensor with components*

$$\beta_{jk} = \int\limits_{Y_p} \frac{d}{|Y_p|}\left(\delta_{jk} + \frac{\partial a_j}{\partial y_k}\right) dy \quad \text{for } j,k = 1,2, \tag{1.13}$$

where for $j = 1,2$, (a_j) *is the solution of the cell-problem*

$$-\nabla_y \cdot (D\,(\nabla_y a_j(y) + e_j)) = 0 \quad \text{for} \quad y \in Y_p, \tag{1.14}$$

$$-D\,(\nabla_y a_j(y) + e_j) \cdot \vec{n} = 0 \quad \text{for} \quad y \in \Gamma, \tag{1.15}$$

$$y \mapsto a_j(y) \text{ is } Y\text{-periodic.} \tag{1.16}$$

We note that u_ε is strongly convergent (up to a subsequence) to a limit $u \in L^2(S\times\Omega)^I$, i.e., $\lim\limits_{\varepsilon\to 0} ||u_\varepsilon - u||_{L^2(S\times\Omega)^I} = 0 \iff \lim\limits_{\varepsilon\to 0} ||u_{\varepsilon_i} - u_i||_{L^2(S\times\Omega)} = 0$ for all i.

2. SIMULATION OF THE MODEL

The physics setting: Let us consider a domain $\Omega := [0,1.2]\times[0,1]$ in $\mathbb{R}^2$. Assume that $Y = [0,1]\times[0,1] \subset \mathbb{R}^2$ is the representative cell with $Y_s := \mathrm{B}((0.5,0.5),0.15)$ as the solid inclusion.[1] Suppose that four mobile species A, B, M and N are present inside Ω. The chemical species diffuse and react with each other (cf. Fig. 2.1).

The reaction is reversible and is given by

$$2\mathrm{A} + 3\mathrm{B} \rightleftharpoons \mathrm{M} + 2\mathrm{N}. \tag{2.1}$$

The stoichiometric coefficients are -2, -3, 1 and 2, and the reaction rates for each species can be given by (1.6). Here $I = 4$ and $J = 1$.

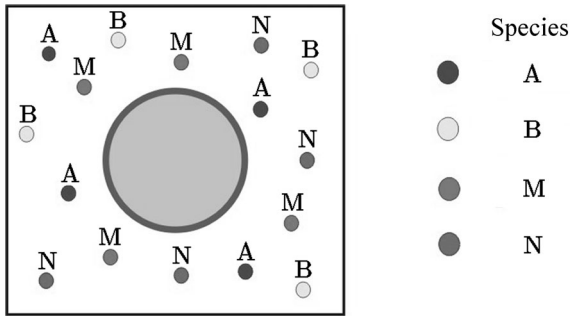

Fig. 2.1. Diffusion-reaction of species A, B, M, and N.

[1] For $r \in \mathbb{R}^n$, $\mathrm{B}(r,\epsilon)$ denotes an open ball centered at r and radius ϵ.

2.1. Simulation at the Micro Scale

Let u_{ε_i} denote the molar concentration of ith species for $1 \leq i \leq 4$. We choose the scaling parameter $\varepsilon = 0.2$. Also, let $D = 1.0$, $k_j^f = 1.8$, $k_j^b = 12.2$. Initially, let us assume $u_{\varepsilon_1}(0, x_1, x_2) = u_1(0, x_1, x_2) = 5x_1$, $u_{\varepsilon_2}(0, x_1, x_2) = 2(x_1 + 3)$, $u_{\varepsilon_3}(0, x_1, x_2) = 5x_1$, and $u_{\varepsilon_4}(0, x_1, x_2) = 2x_1$.

We choose "coarser" mesh available in COMSOL to discretize the domain Ω_p^ε. The triangulization of the domain Ω_p^ε is depicted in Fig. 2.2.

We solve the system of diffusion-reaction equations at the micro scale for $t = 10$ s. We notice that: the number of elements for mesh is 4930, the number of degrees of freedom is 10640 and the time taken by

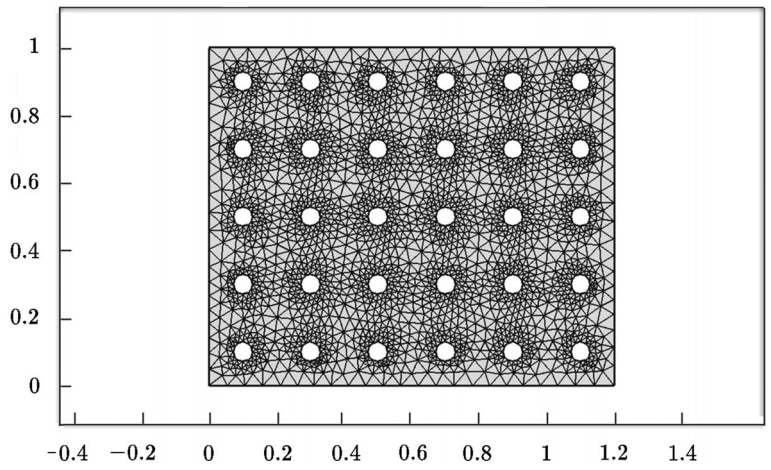

Fig. 2.2. The triangulization of Ω_p^ε for $\varepsilon = 0.2$.

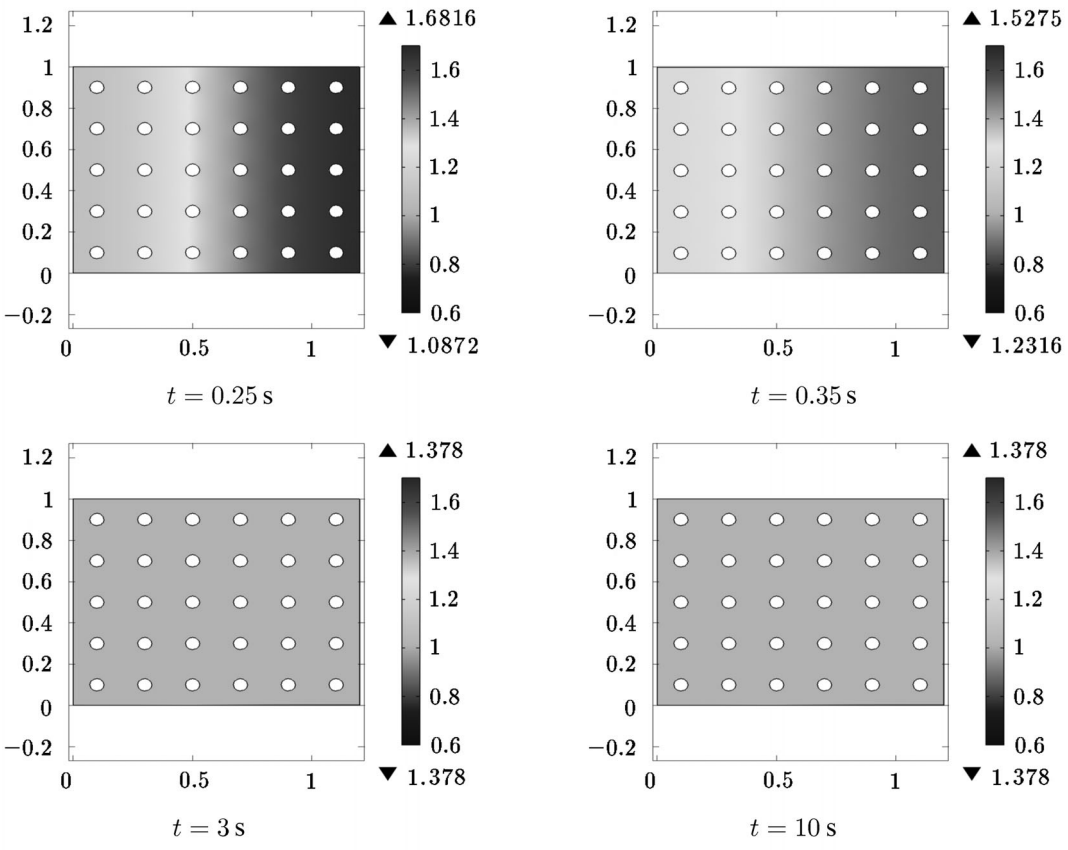

Fig. 2.3. Concentration of species A in Ω_ε^p at different time.

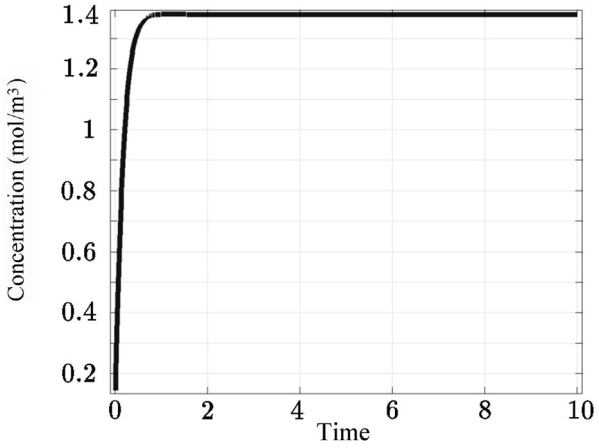

Fig. 2.4. Concentration of species A at the point $(0, 1)$ in Ω_p^ε in 10 s.

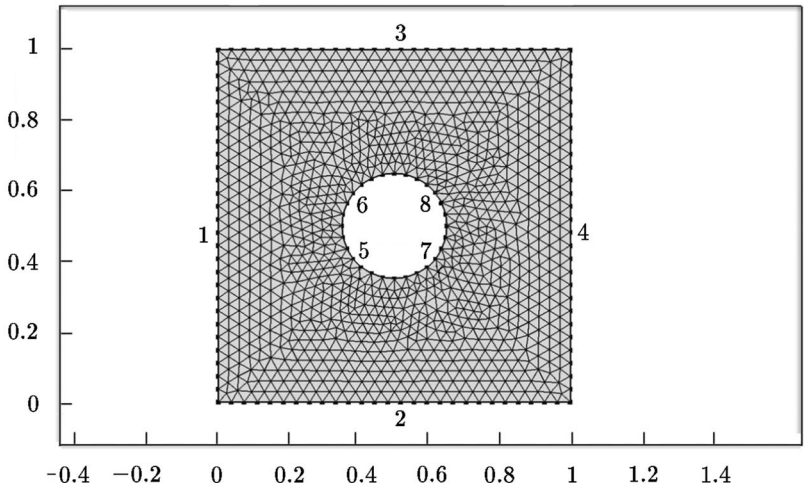

Fig. 2.5. The triangulization of cell Y.

the solver is 104 s. However, here we compare the solution for species A only at the micro and the macro scale, since the comparison of the solutions for the rest of the species can be done analogously. The molar concentration of species A is depicted in Fig. 2.3 for $t = 0.25$ s, $t = 0.35$ s, $t = 3$ s, and $t = 10$ s, respectively.

In Fig. 2.3, we see the change in concentration of species A at different times. As the time progesses, the concentration of species A increases and due to reversible reaction after $t = 3$ s, the reaction reaches equilibrium. This is also shown in Fig. 2.4 where the concentration of species A at the point $(0, 1)$ in Ω_p^ε is plotted. Now we compute the effective diffusive tensor for species A. We commence by solving the cell-problems (1.14)–(1.16) in Y.

2.2. Solution of the Cell-Problems

We choose the "finer mesh option" (available in COMSOL) for the triangulization of the cell Y. The triangulization of Y is depicted in Fig. 2.5.

In Fig. 2.6 we see the solution of the cell-problems.

With the help of "derived values" feature in COMSOL, we compute the diffusive tensor by formula (1.13). Thus we obtain

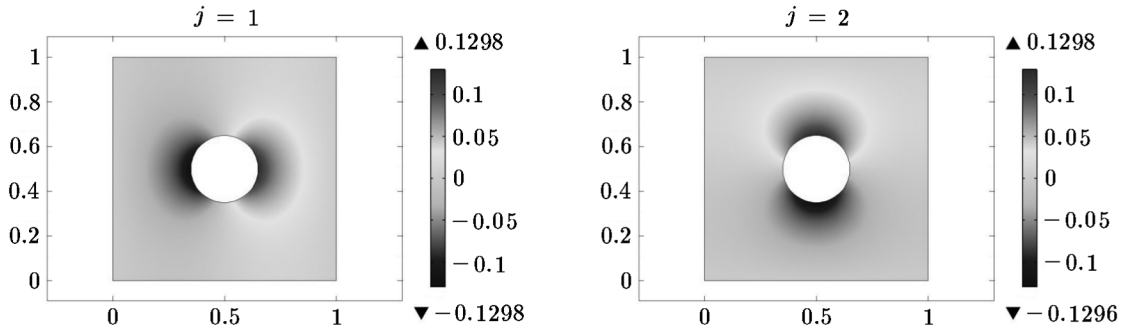

Fig. 2.6. Solution a_j of the cell-problem for $j = 1, 2$.

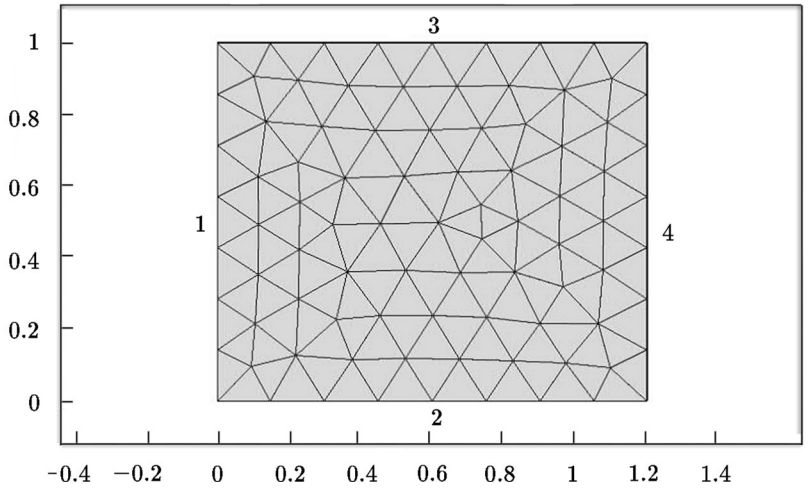

Fig. 2.7. The triangulization of Ω.

$$P = (p_{jk})_{\substack{1\le j\le 2\\ 1\le k\le 2}} = \begin{bmatrix} 0.93409 & 4.19\times 10^{-7} \\ 4.19\times 10^{-7} & 0.93409 \end{bmatrix}. \tag{2.2}$$

2.3. Simulation at the Macro Scale

For the simulation of upscaled model, we choose P from (2.2), $k_j^f = 1.8$ and $k_j^b = 12.2$. Initially, $u_1(0, x_1, x_2) = 5x_1$, $u_2(0, x_1, x_2) = 2(x_1 + 3)$, $u_3(0, x_1, x_2) = 5x_1$, and $u_4(0, x_1, x_2) = 2x_1$. We choose "coarser mesh" (in COMSOL) for Ω with 144 elements. The descritization of the domain Ω is depicted in Fig. 2.7.

We also notice that the number of degrees of freedom is 352 and the time taken by the solver is 11 s. The numerical simulations are shown in Figs. 2.8 and 2.9.

3. CONCLUSIONS

Firstly, we notice that for the same type of mesh the solver takes less time to solve the macro problem than to solve the micro problem. Therefore, the upscaled model is computationally efficient. In Fig. 2.8, it is shown that as the time progresses, there is an increase in the concentration of species A and after $t = 2.4$ s the reaction reaches equilibrium as expected. By comparing Figs. 2.3 and 2.8, we can notice that the upscaled model (1.10)–(1.12) is an approximation to our original micro problem (1.1)–(1.4).

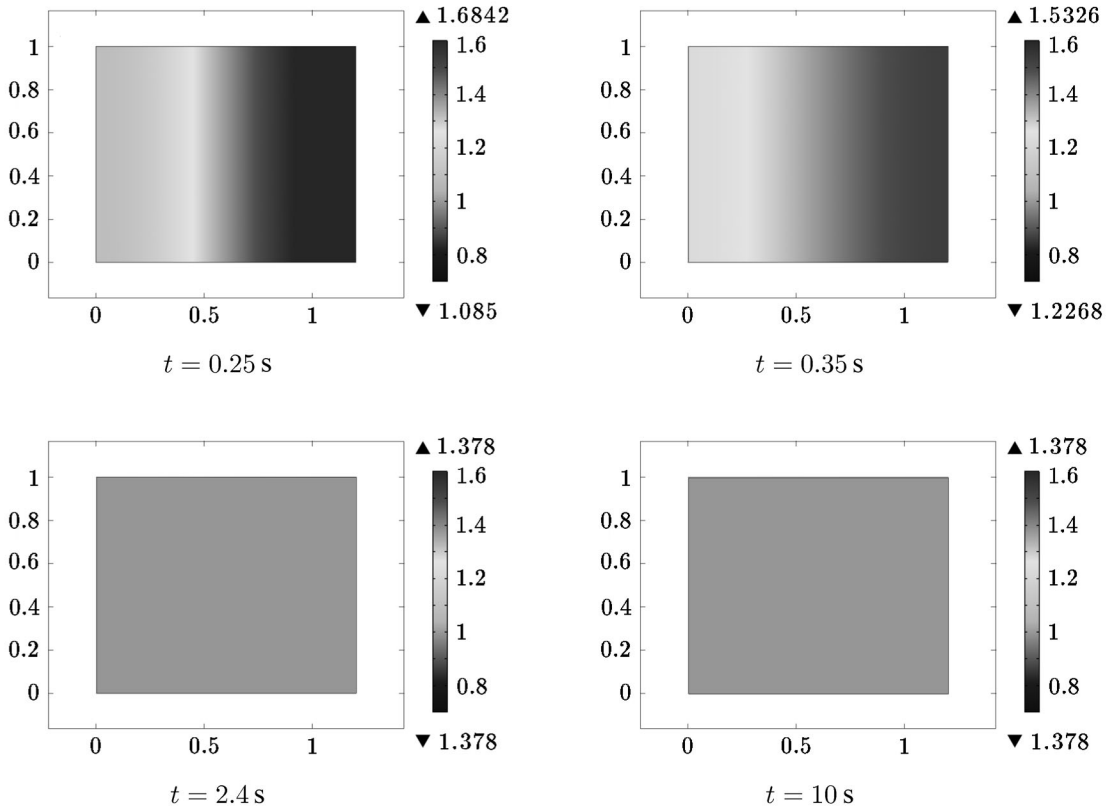

Fig. 2.8. Concentration of species A in Ω at different time scales.

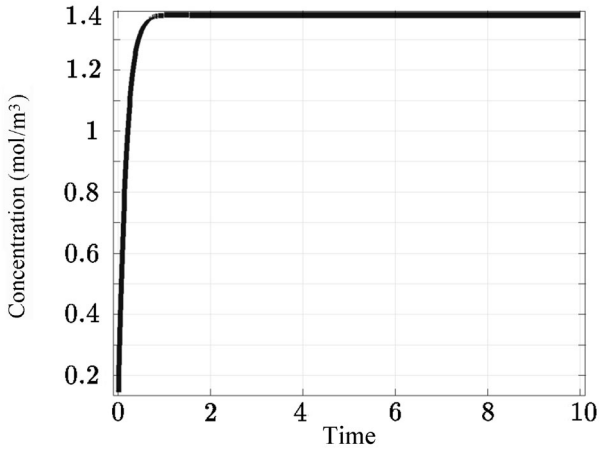

Fig. 2.9. Concentration of species A at the point $(0, 1)$ in Ω in 10 s.

This can also be seen by comparing Figs. 2.4 and 2.9. Moreover, using the features of COMSOL, we can compute

$$||u_{\varepsilon_\mathrm{A}} - u_\mathrm{A}||_{L^2(S\times\Omega)} = \int\limits_{S\times\Omega} |u_{\varepsilon_\mathrm{A}} - u_\mathrm{A}|^2 \, dx \, dt = 0.432 \times 10^{-6},$$

where u_A is the concentration of species A.

Thus, the upscaled model gives us the global information (behaviors) of the properties related to chemical transport in the porous medium, which was microscopically heterogeneous. By homoge-

nization we have obtained a mathematical model that does not involve any heterogeneities, which is an approximation to the micro model and takes less time to compute. Therefore, homogenization techniques are proven to be a nice tool to deal with such kind of problems.

ACKNOWLEDGMENTS

The author is grateful to the Center of Industrial Mathematics located at the University of Bremen for providing a nice working environment during his stay there.

REFERENCES

1. *Comsol User's Guide*, COMSOL Multiphysics, 2010.
2. Bothe, D. and Rolland, G., Global Existence for a Class of Reaction-Diffusion Systems with Mass Action Kinetics and Concentration-Dependent Diffusivities, *Acta Appl. Math.*, 2015, vol. 139, pp. 25–57.
3. Mahato, H.S. and Böhm, M., Global Existence and Uniqueness for a System of Nonlinear Multi-Species Diffusion Reaction Equations in an $H^{1,p}$ Setting, *J. Appl. An. Comput. (JAAC)*, 2013, vol. 3, no. 4, pp. 357–376.
4. Mahato, H.S. and Böhm, M., Homogenization of a System of Semilinear Diffusion-Reaction Equations in an $H^{1,p}$ Setting, *El. J. Diff. Eq. (EJDE)*, 2013, vol. 210, pp. 1–22.
5. Marion, M. and Temam, R., Global Existence for Fully Nonlinear Reaction-Diffusion Systems Describing Multicomponent Reactive Flows, *J. Math. Pure Appl.*, 2015, vol. 104, pp. 102–138.
6. Meirmanov, A. and Zimin, R., Compactness Result for Periodic Structures and Its Application to the Homogenization of a Diffusion-Convection Equation, *El. J. Diff. Eq. (EJDE)*, 2011, vol. 115, pp. 1–11.
7. Pierre, M., Global Existence in Reaction-Diffusion Systems with Control of Mass: A Survey, *Milan J. Math.*, 2010, vol. 78, no. 2, pp. 417–455.
8. Prüss, J. and Schnaubelt, R., Solvability and Maximal Regularity of Parabolic Evolution Equations with Coefficients Continuous in Time, *J. Math. An. Appl.*, 2001, vol. 256, pp. 405–430.
9. Rubin, J., Transport of Reacting Solutes in Porous Media: Relation between Mathematical Nature of Problem Formulation and Chemical Nature of Reactions, *Water Resour. Res.*, 1983, vol. 19, no. 5, pp. 1231–1252.